E&G Quaternary Science Journal
Volume 60 / Number 1 / 2011 / 105–115 / DOI 10.3285/eg.60.1.07
www.quaternary-science.net

GEOZON SCIENCE MEDIA
ISSN 0424-7116

IRSL Signals from Maar Lake Sediments Stimulated at Various Temperatures

Esther Dorothe Schmidt, Andrew S. Murray, Frank Sirocko, Sumiko Tsukamoto, Manfred Frechen

Abstract: Optically stimulated luminescence (OSL) and infrared stimulated luminescence (IRSL) have been measured from seven fine-grained samples from core JW3 from the dry maar of Jungfernweiher (West Eifel /Germany). Two different elevated temperature post-IR IRSL protocols in the blue detection were applied to polymineral fine grains (4–11 µm). These protocols involve stimulation with IR for up to 200s at 50°C prior to elevated temperature stimulation with IR for 100s at 225°C or 200s at 290°C. Quartz OSL saturates at doses of 260–300 Gy, and the D_e values obtained using IRSL at 50°C (IR_{50}) do not increase with depth indicating that this signal is also in field saturation at ~500 Gy. However, the post-IR IRSL signals at 225°C ($pIRIR_{225}$) and 290°C ($pIRIR_{290}$) increase with depth from ~800 Gy to ~1400 Gy, suggesting a minimum (fading uncorrected) age of ~200 ka for the youngest sediments. Mean laboratory fading rates are 4.09 ± 0.02%/decade for IR_{50} and 2.55 ± 0.14%/decade for polymineral $pIRIR_{225}$. For sample JWS1 a g-value of 0.52 ± 1.12%/decade for the $pIRIR_{290}$ was obtained. Both fading corrected $pIRIR_{225}$ and uncorrected $pIRIR_{290}$ D_e values from the youngest sample (~16 m below modern surface) indicate an age estimate of ~250 ka for the uppermost sample increasing up to ~400 ka for the oldest samples taken ~94 m below modern surface.

[IRSL Signale von Maarseesedimenten stimuliert mit verschiedenen Temperaturen]

Kurzfassung: Optisch stimulierte Lumineszenz (OSL) und infrarot stimulierte Lumineszenz (IRSL) wurden an sieben Feinkorn Proben von Kern JW3 aus dem Trockenmaar Jungfernweiher gemessen. Zwei verschiedene post-IR IRSL Messprotokolle (blaue Detektion) wurden an den polymineralischen Feinkörnern (4–11 µm) angewandt. Diese Protokolle beinhalten eine Stimulation mit IR bei 50°C für bis zu 200 s vor einer weiteren IR Stimulation bei erhöhten Temperaturen bei 225°C für 100 s oder 290°C für 200 s. Die OSL von Quarz sättigt bei Dosen von 260–300 Gy und die De-Werte, die mit IRSL bei 50°C (IR_{50}) erhalten werden, nehmen mit der Tiefe nicht zu. Dies weist darauf hin, dass auch dieses Signal bei ~500 Gy in Sättigung geht. De-Werte des post-IR IRSL Signals bei 225°C ($pIRIR_{225}$) und 290°C ($pIRIR_{290}$) nehmen jedoch mit der Tiefe von ~800 Gy bis ~1400 Gy zu, und zeigen ein korrigiertes Minimalalter von ~200 ka für die jüngsten Sedimente an. Die durchschnittlichen im Labor gemessene Fadingraten liegen für IR50 bei 4.09 ± 0.02%/decade und für $pIRIR_{225}$ bei 2.55 ± 0.14%/decade. Für Probe JWS1 wurde für $pIRIR_{290}$ ein g-value von 0.52 ± 1.12%/decade gemessen. Sowohl fading korrigierte $pIRIR_{225}$ als auch unkorrigierte $pIRIR_{290}$ D_e-Werte der jüngsten Probe (~16 m unterhalb der heutigen Erdoberfläche) weisen auf ein Alter von ~250 ka für die oberste Probe hin. Für die ältesten Proben, die in ~94 m unterhalb der heutigen Erdoberfläche genommen wurden, wurden Alter von bis zu ~400 ka gemessen.

Keywords: *luminescence dating, IRSL, OSL, fading, fine grain, maar lake, Jungfernweiher, ELSA*

Addresses of authors: **E. D. Schmidt***, **S. Tsukamoto**, **M. Frechen**, Leibniz Institute for Applied Geophysics (LIAG), Section 3: Geochronology and Isotope Hydrology, Stilleweg 2, 30655 Hannover, Germany. E-Mail: Esther.Schmidt@liag-hannover.de, EstherDorothe.Schmidt@googlemail.com; **E. D. Schmidt**, **A.S. Murray**, Nordic Laboratory for Luminescence Dating, Department of Earth Sciences, Aarhus University, Risø DTU, DK-4000 Roskilde, Denmark; **F. Sirocko**, University of Mainz/Germany, Institute for Geoscience. **corresponding author*

1 Introduction

Maars are volcanic craters caused by phreatomagmatic eruptions. Volcanic depressions and craters such as those of maar lakes form excellent sediment traps, and so can record past climatic and environmental changes. Sediments accumulating in maar lakes are often thought to have undergone continuous deposition since the eruption of the maar volcanoes, and hence may contain unique continuous local records of climate change. Aeolian dust (loess) can make up a large part of the sediment inventory, because the catchment surrounding the lake often only extends to the rim of the crater. Because of its more or less continuous supply during cold periods, loess is one of the most detailed and wide-spread terrestrial archives of climate and environment change. As a result it often provides information on local and regional environmental processes and conditions for the Middle and Late Pleistocene. The West Eifel volcanic field (Fig.1) contains dry maars, maar lakes, scoria cones and small stratovolcanoes. The Jungfernweiher is one of about 60 dry maars; with a diameter of 1500 m it is the biggest maar in the Eifel area. Nowadays there is a pond in the dry maar lake (Schaber & Sirocko, 2005). Sediment cores have been drilled within the framework of the ELSA project (Eifel Laminated Sediment Archive) in Eifel dry maar lakes (Sirocko et al. 2005), and samples for luminescence dating were taken from core JW3 and JW2 from the Jungfernweiher.

Luminescence dating is used to date the time that has passed since the last exposure of minerals (quartz or feldspar) to daylight (Aitken, 1998). Such minerals are able to store energy (as trapped electrons) within their crystal structure; this energy originates from ionising radiation (alpha, beta and gamma) from environmental radioactivity,

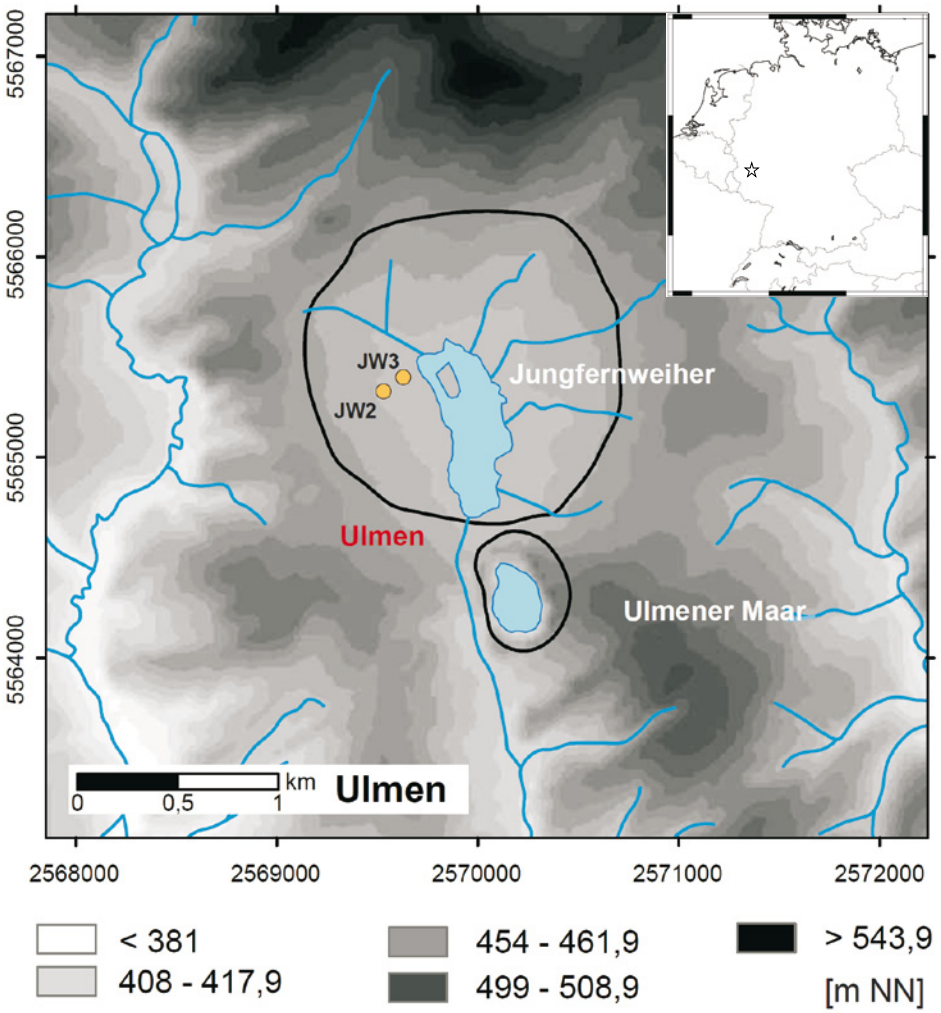

Fig. 1: Map showing coring locations of the dry maar of Jungfernweiher, West Eifel Volcanic Field.

Abb. 1: Lage der Bohrpunkte des Trockenmaars Jungfernweiher, Vulkanfeld der Westeifel.

and from cosmic rays. The trapped electrons can be stored for long periods at lattice defects in the crystal lattice. In the laboratory the grains are stimulated with light and the trapped electrons are released. During recombination they release their stored energy as light (luminescence). A measurement of this luminescence allows an estimation of the radiation dose (palaeodose or equivalent dose, D_e) that the crystal has absorbed since the last exposure to daylight. The most important requirement is that the sediments are well bleached or zeroed at the time of deposition due to a sufficient exposure to daylight. For loess it is expected that any residual trapped charge has been completely removed during the long aeolian transport. The optically stimulated luminescence (OSL) of quartz has been widely used to estimate the deposition age of sediments and is usually regarded as an accurate and precise dating method (e.g. Murray & Olley, 2002). However, the fast component of the quartz OSL signal (the component normally used for dating) saturates at doses of 200–400 Gy (Wintle & Murray, 2006). This implies a quartz upper age limit of ~50–70 ka for loess deposits for a typical dose rate of between 3 and 4 Gy/ka (e.g. Frechen, 1992, Roberts, 2008, Schmidt et al., 2011).

In contrast, the infrared stimulated luminescence (IRSL) signals from feldspars grow to much higher doses than those from quartz, and this offers the possibility of significantly extending the age range. Several studies report the application of luminescence to limnic sediments (e.g. Degering & Krbetschek, 2007b), but infrared stimulated luminescence (IRSL) on maar sediments has only been used in a few studies (e.g. Lang & Zolitschka, 2001, Degering & Krbetschek, 2007a). Lang & Zolitschka (2001) obtained reliable IRSL ages only for clastic-rich horizons; IRSL ages of sediments with high concentrations of biogenic material were inaccurate. Degering & Krbetschek (2007a) provided two IRSL ages (multiple aliquot additive dose protocol, MAAD) from the Jungfernweiher.

Luminescence dating of feldspars tends to underestimate the age, because of anomalous fading (Wintle, 1973) caused by quantum-mechanical tunnelling (Visocekas, 1985). Feldpar dating is normally carried out using a 50° C IR stimulation with detection in the blue (-violet) spectrum. Many studies have shown that the IRSL ages without fading correction consistently underestimate quartz OSL ages (e.g. Schmidt et al., 2010) due to anomalous fading. Hence the fading rate (g-value; Aitken, 1985) has to be determined in the laboratory and the ages corrected for this effect. Several methods of age corrections have been proposed (e.g. Huntley & Lamothe, 2001; Lamothe et al., 2003) and many studies give corrected IRSL ages which are in good agreement with quartz OSL ages. However, there is no ge-neral consensus as to which correction method should be used and the most commonly adopted method is only valid for the 'linear part' of the dose response curve (Huntley & Lamothe, 2001). Clearly, if the fading rate could be reduced, feldspar dating would be more

E&G / Vol. 60 / No. 1 / 2011 / 105–115 / DOI 10.3285/eg.60.1.07 / © Authors / Creative Commons Attribution License

reliable. Thomsen et al. (2008) found out that stimulation at elevated temperatures significantly reduces the fading rate. Based on this study Buylaert et al. (2009) tested a SAR protocol with detection in the blue (320–460 nm); this involves a stimulation with IR for 100s at 50°C prior to an elevated temperature stimulation with IR for 100s at 225°C, a so called post-IR IRSL measurement sequence. They have shown that the observed fading rates for the post-IR IRSL signal are significantly lower than those from the conventional IRSL at 50°C and that the signal is bleachable in nature. Thiel et al. (2011) extended this investigation following the observation of Murray et al. (2009) that the IR dosimetry trap lies above 320°C, and hence preheat temperatures up to this temperature can be used. In their study they chose a preheat of 320°C (60s) and a stimulation temperature of 290°C (200s) for the post-IR IRSL signal. They found natural signals from a sample below the Brunhes/Matuyama boundary in saturation on a laboratory growth curve and they concluded that they were unable to detect fading in this field sample.

The aim of this study is to investigate the applicability of luminescence dating using maar sediments, and ultimately to determine the accumulation rate of sediments within the archive and temporal succession of dust storms. The different IRSL signals are compared and discussed in regard to their performance in SAR; the equivalent doses (D_e) and the fading rates are then determined and ages calculated. The IRSL signal measured at 50°C and the subsequent post-IR IRSL signals measured at 225°C and 290°C are hereafter referred to as IR_{50}, $pIRIR_{225}$ and $pIRIR_{290}$ respectively. The results are discussed in terms of continuity of sedimentation and sedimentation rates.

2 Geological setting

The West Eifel volcanic field/Germany with an aerial extension of 600 km^2 is aligned NW-SE from Ormont to Bad Bertrich in Rhineland Palatinate, i.e. west of the river Rhine. Volcanism in the West Eifel Area started ca. 700 ka ago producing 250 eruptive centers with more than 50 maars, of which 8 are still filled with water (Büchel, 1984, Negendank & Zolitschka, 1993).

Sediment cores have been drilled by the ELSA project (Eifel Laminated Sediment Archive) in Eifel dry maar lakes to reconstruct the palaeoclimatic and palaeoenvironmental conditions as well as the history of the volcanism in the Eifel/Central Europe during the last glacial cycles. Two drillings (JW2 and JW3) have been carried out at the Jungfernweiher. JW3 was drilled close to center of the maar and exhibits a more undisturbed sedimentation and a better core quality than core JW2 which is located closer to the edge of the maar (Schaber & Sirocko, 2005). Seven samples for luminescence dating were taken from core JW3. According to Schaber & Sirocko (2005) coversand and loess layers were accumulated during high-glacial conditions and during cold phases rhythmic stratification of clay and silt was dominating. All samples were taken from a glacial cycle with mainly silt lamination. Additionally, one sample was taken from the drill core JW2. The sampled material consists of loessic gyttja with intercalated small bands of coarser silty to sandy material, which is supposed to originate from dust storms. Some independent age control is provided by 16 radiocarbon age estimates. However, the uncalibrated ages range from 35 ± 2 ka to 56 ± 4 ka and do not increase with depth. A study carried out by Lenaz et al. (2010) presents mineralogical data from core JW3 suggesting that the tephra layer at a depth of 107.39 m could be correlated with the Rocourt Tephra which has an age range between 90.3 and 74 ka (Pouclet et al., 2008). Luminescence dating was carried out by Degering & Krbetschek (2007a) on two samples with a depth of 104.5 m and 122.5 m from core JW2. They applied a multiple aliquot additive dose (MAAD) protocol on the polymineral fine-grain fraction and could not detect anomalous fading for their samples. They obtained equivalent doses (D_e) of 441 ± 49 Gy and 517 ± 62 Gy and calculated ages of 98 ± 15 ka and 117 ± 18 ka.

3 Experimental details

Samples were extracted under subdued red light and pretreated with 10% hydrochloric acid to remove carbonates, sodium oxalate to dissolve aggregates and 30% hydrogen peroxide to remove organic matter. The 4–11 µm silt fraction was separated and divided into two parts: (i) an untreated fraction used for polymineral infrared stimulated luminescence (IRSL) measurements, and (ii) a fraction from which quartz grains were extracted. The latter polymineral fraction was treated with 34% fluorosilicic acid (H_2SiF_6) for 6 days, preferentially dissolving feldspar grains, and leaving behind a quartz-rich extract. Finally, samples were prepared for measurement by settling either the polymineral or the quartz grains (4–11 µm) from acetone onto aluminium discs. The purity of the quartz extract was checked using the IR depletion ratio (Duller, 2003). All OSL/IRSL measurements were performed using an automated Risø TL/OSL-DA20 equipped with a $^{90}Sr/^{90}Y$ beta source. Quartz blue-stimulated OSL was measured for 40 s at 125°C and the signals were detected through 7.5 mm of Hoya U-340 filter (passing from 260 to 390 nm, i.e. UV). Feldspar IRSL was detected through Schott BG-39 and Corning 7-59 filters (passing from 320 to 460 nm; i.e. blue). For measurement of the equivalent dose (D_e) of quartz fine-grains a conventional SAR protocol (Murray & Wintle, 2000) was applied. The signal was integrated over the initial 1 s of stimulation, and a background based on the last 5 s of simulation subtracted. D_e estimates from polymineral fine-grains were determined using a post-IRSL elevated-temperature IR SAR protocol.

Radionuclide concentrations for all samples were obtained using high-resolution gamma spectrometry of sediment collected from the immediate surrounding of the samples. A water content of 20 ± 5 % was estimated for all samples. To derive the effective alpha dose rate, mean a-values of 0.04 ± 0.02 for quartz OSL and of 0.08 ± 0.02 for polymineral IRSL were assumed (Rees-Jones, 1995). The uranium, thorium, potassium contents and the dose rate of the samples are summarised in Table 1. The concentrations of uranium, thorium and potassium were converted into infinite-matrix dose rates using the conversion factors of Adamiec & Aitken (1998) and water-content attenuation factors (Aitken, 1985). Estimation of the cosmic-ray dose rate was calculated according to Prescott & Stephan (1982) and Prescott & Hutton (1994) from a knowledge of burial depth, altitude, matrix density, latitude and longitude for

Tab. 1: Dose rate data from potassium, uranium and thorium content, as measured by gamma spectrometry.

Tab. 1: Dosimetrische Ergebnisse basierend auf Kalium, Uran und Thorium Gehalt (gemessen mit Gammaspektrometrie).

Sample	Uranium [ppm]	Thorium [ppm]	Potassium [%]	IRSL dose rate [Gy/ka]	OSL dose rate [Gy/ka]
JWS1	2.78 ± 0.04	13.33 ± 0.10	2.49 ± 0.02	4.25 ± 0.21	3.85 ± 0.21
JWT3	2.90 ± 0.04	14.22 ± 0.12	2.59 ± 0.03	4.44 ± 0.21	4.02 ± 0.22
JWT9	2.85 ± 0.04	14.56 ± 0.04	2.76 ± 0.03	4.60 ± 0.23	4.18 ± 0.23
JWT5	3.03 ± 0.04	11.85 ± 0.09	1.91 ± 0.02	3.70 ± 0.19	3.31 ± 0.19
JWT7	2.67 ± 0.04	11.59 ± 0.10	1.81 ± 0.02	3.96 ± 0.20	3.65 ± 0.20
JWS8	3.43 ± 0.05	11.81 ± 0.12	1.55 ± 0.03	3.51 ± 0.18	3.09 ± 0.18
JWT8	3.21 ± 0.04	11.55 ± 0.10	1.74 ± 0.02	3.58 ± 0.18	3.18 ± 0.18
JWT9	3.17 ± 0.05	13.27 ± 0.08	2.22 ± 0.02	4.04 ± 0.21	3.67 ± 0.21

each sample. The uranium, thorium, potassium content and total dose rates are shown in Table 1. The mean dose rate is 3.61 ± 0.15 Gy/ka for quartz and 4.01 ± 0.15 Gy/ka for polymineral samples.

4 Luminescence dating

4.1 OSL dating of quartz

To test the suitability of the SAR protocol to the samples from the Jungfernweiher, and to confirm the most appropriate preheat temperature, the dose recovery ratio (Murray & Wintle, 2003) was determined for preheat temperatures between 200 and 260°C for 10 s following all natural and regeneration doses, and 200°C for 1 s following all test doses, using sample JWS 1. The aliquots were first bleached twice with 1000 s blue stimulation at room temperature separated by a 5000 s pause to allow the decay of any charge transferred to the 110°C TL trap, before giving a dose approximately equal to the natural dose. This dose was then measured in the same manner as if measuring the equivalent dose to provide confirmation that the protocol is able to recover a known dose successfully. If the SAR protocol is appropriate for our samples, the measured to given dose ratio should be close to unity. The measured dose/given dose ratio is close to unity for preheat temperatures of 220°C and 240°C (0.99 ± 0.01). We chose a preheat temperature of 240°C for our measurements. Fig. 2 shows the dose response curve for sample JWS1. This curve is representative for all measured samples. Fine-grain equivalent doses (D_e) were measured for samples JWS1, JWT3 and JWT7 and range from 440 ± 30 Gy to 580 ± 40 Gy (Table 3); the D_0-values for all samples are about ~130-150 Gy, when the dose response curve is fitted to a single saturating exponential plus linear function,

$$I = I_{max} (1-\exp(-D/D_0)) + kD,$$

(1) where I is the sensitivity corrected OSL intensity, I_{max} is saturation intensity of OSL, D is dose, and D_0 is the characteristic saturation dose.

Wintle & Murray (2006) suggested equivalent dose (D_e) values should only be reported up to ~$2D_0$. In our case it should therefore be possible to measure doses up to about ~260–300 Gy using our material, although the laboratory-generated dose response curves continue to grow up to ~ 1000 Gy, because of a more slowly saturating component which is expressed by the linear term in equation 1. Buylaert et al. (2007), Timar et al. (2010) and Lowick et al. (2010a,b) made similar observation for their fine-grain quartz samples and concluded that equivalent doses larger than $2D_0$ (~120-140 Gy) were not very reliable. At doses higher than this value they observed an increasing age underestimation towards the Eemian. The samples described by Lowick et al. (2010b) passed all standard performance criteria and still show an increasing dose response curve at 500 Gy. Taking all these observations into account, we consider our quartz fine-grain equivalent doses to be in or close to saturation, and conclude that they provide a minimum dose estimate of ~450 Gy for the youngest sample.

4.2 IRSL dating of polymineral fine-grains

Post-IR IRSL measurement sequence

Based on the work of Thomsen et al. (2008), Buylaert et al. (2009) proposed a new SAR protocol, with detection in the blue (320–460 nm). This protocol involved elevated temperature stimulation with IR for 100 s at 225°C ($pIRIR_{225}$), following stimulation with IR for 100 s at 50°C, a so-called post-IR IRSL measurement sequence (Table 2), and these authors chose a preheat of 250°C to make their results comparable to other studies. Recently Thiel et al. (2011) used a preheat of 320°C for 60 s for their post-IR IRSL protocol and used a stimulation at 290°C for 200 s after bleaching the aliquots with IR diodes at 50°C for 200 s to date polymineral fine-grains. Buylaert et al. (2009) showed that the observed fading rates for their post-IR IRSL signal (stimulated at 225°C) were significantly lower than from the conventional IR_{50} and that the signal is bleachable in nature. Thiel et al. (2011) reported

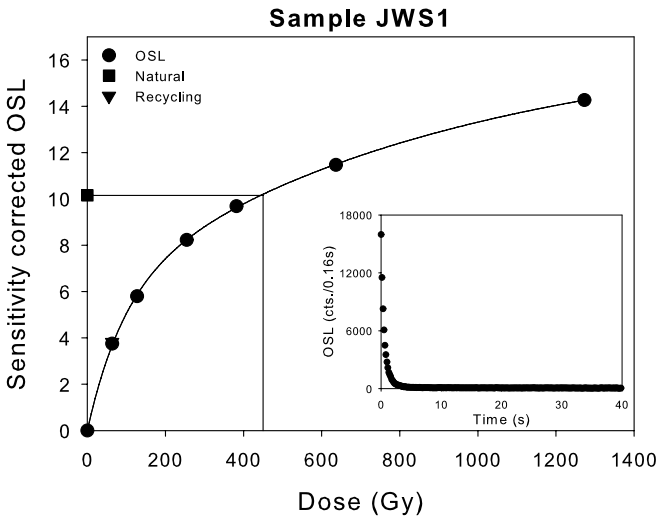

Fig. 2: Dose response and decay curve for sample JWS1 showing the OSL from fine grain quartz.

Abb. 2: Aufbaukurve und Zerfallskurve für Probe JWS1 für OSL von Feinkorn Quarz.

Tab. 2: Elevated temperature post-IR IRSL measurement sequence.

Tab. 2: Post-IR IRSL Messprotokoll.

Step	Treatment	Observed
1	Dose	
2	Preheat, 60s at 250°C / 60s at 320°C	
3	IR stimulation, 100s at 50°C / 200s at 50°C	Lx
4	IR stimulation, 100s at 225°C / 200s at 290°C	Lx
5	Test dose	
6	Preheat, 60s at 250°C / 60s at 320°C	
7	IR stimulation, 100s at 50°C / 200s at 50°C	Tx
8	IR stimulation, 100s at 225°C / 200s at 290°C	Tx
9	IR stimulation, 40s at 290°C / 40s at 325°C	
10	Return to step 1	

natural signals in saturation on the laboratory growth curve and concluded that fading is negligible for their samples.

In this study, the $pIRIR_{225}$ protocol is applied to polymineral fine-grains from the Jungfernweiher, and in addition the $pIRIR_{290}$ is measured for two samples. The initial 2 s of the post-IR IR signal are used for calculating the D_e values, with a background based on the signal observed in the last 10 s of the decay curve. To test for anomalous fading and to compare the fading rates of the IR_{50}, the $pIRIR_{225}$ and the $pIRIR_{290}$, those aliquots which had been used for D_e measurement were then used to test for fading, by dosing and preheating the aliquots and then storing for various delays after irradiation and before measurement. This sequence was repeated several times on each aliquot. The fading rates are expressed in terms of the percentage decrease of intensity per decade of time (g-value; Aitken, 1985; Auclair et al., 2003). G-values were calculated according to Huntley & Lamothe (2001) using the signal integration limits as for the D_e calculation. Fading corrections use the methods proposed in Huntley & Lamothe (2001); it is recognised that this method is strictly applicable only for natural doses in the linear region of the growth curve, although Buylaert et al. (2008; 2009; in press) have shown that the correction can give accurate ages outside of this range.

Luminescence characteristics and performance in SAR

The dose response curves and the decay curves for IR_{50} and $pIRIR_{225}$ for the uppermost sample JWS1 (~17 m) and for the lowermost sample JWT8 (~94 m) is shown in Fig. 3a,b. The curves are representative for all the other samples measured using the $pIRIR_{225}$. The natural IRSL signal clearly lies below the natural post-IR IRSL signal, by about 15–20% on average. The shapes of the growth curves are similar but the growth curve for IR_{50} tends to lie somewhat above the curve for $pIRIR_{225}$ for all our samples. Fig.4 a, b shows corresponding dose response and decay curves for IR_{50} and $pIRIR_{290}$ for the uppermost sample JWS1 (~17 m) and for one of the lowermost samples JWS8 (~94 m). As for $pIRIR_{225}$, the natural $pIRIR_{290}$ lies clearly above the natural IRSL signal, and the growth curves for IR50 lie somewhat above the curves for $pIRIR_{290}$ for all samples. Fig. 5 a, b show dose response curves and decay curves for IR_{50}, the $pIRIR_{225}$ and $pIRIR_{290}$ for sample JWT9. This is in contrast to the study of Buylaert et al. (2009) who observed that the shape of the growth curves for IR50 and $pIRIR_{225}$ are indistinguishable. Thiel et al. (2011) also investigated IR_{50} and $pIRIR_{290}$ growth curves and observed very similar shapes. In our study, the $pIRIR_{225}$ from all the samples is brighter (~12-20%) than for the IR_{50}. The $pIRIR_{290}$ is ~3 times brighter than for the IR_{50}. Buylaert et al. (2009) and Thiel et al. (this issue) made similar observations. Recycling ratios for our samples range from 0.96 ± 0.01 to 1.02 ± 0.02 for the IR_{50} and from 0.95 ± 0.02 to 0.98 ± 0.01 for $pIRIR_{225}$. Recuperation for all the IRSL, $pIRIR_{225}$ and $pIRIR_{290}$ signals is below 5% of the natural signal. To test the applicability of the post-IR IRSL protocol using a stimulation temperature of 225°C, the dose recovery ratio was measured for all samples (Murray & Wintle, 2003). The aliquots were bleached for 4 hours in a Hönle SOL2 solar simulator before giving a dose approximately equal to the natural dose. Fig. 6a shows the results of the dose recovery test for all samples for IR_{50} and $pIRIR_{225}$. The mean ratio of the measured to given dose is 1.060 ± 0.011, n = 21 for IR_{50} and 0.98 ± 0.006, n = 21 for $pIRIR_{225}$ confirming the suitability of our post-IR IRSL protocol. To confirm that IRSL and post-IR IRSL signals are bleachable by natural daylight we exposed three aliquots per sample for four hours to a Hönle SOL2 solar simulator and then measured the apparent dose in the usual manner. The results are shown in Fig. 6 b. The residual doses range from 2.21 ± 0.13 Gy to 2.84 ± 0.01 Gy, with a mean of 2.37 ± 0.15 Gy (n = 18) for IR_{50} and from 3.92 ± 0.51 Gy to 5.54 ± 0.91 Gy, with a mean of 4.88 ± 0.19 Gy (n = 19) for $pIRIR_{225}$. The residual doses were subtracted from the measured equivalent doses (D_e) for age calculation.

a)

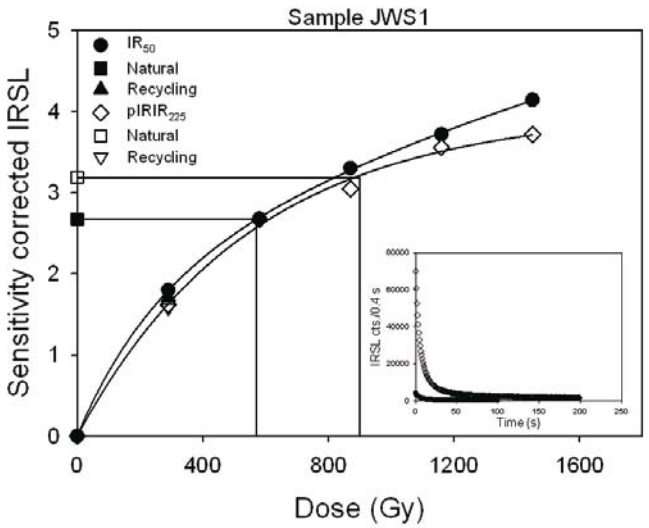

b)

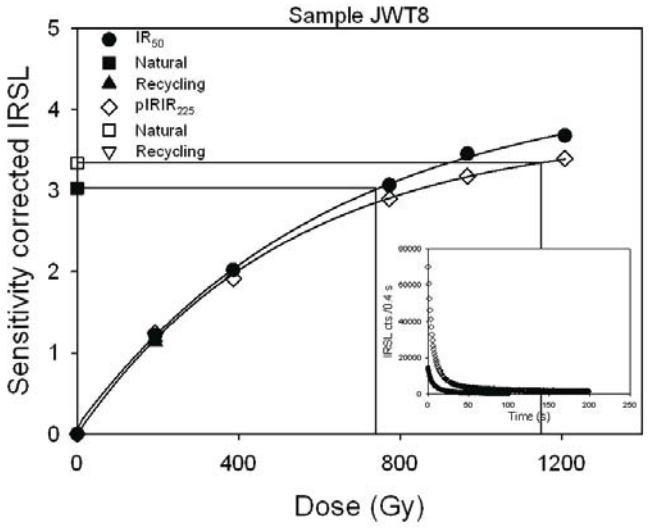

Fig. 3: Dose response and decay curves for sample a) JWS1 and b) JWS8 showing the IR_{50} (filled symbols) and the $pIRIR_{225}$ (open symbols).

Abb. 3: Aufbaukurve und Zerfallskurve für Proben a) JWS1 (gefüllte Symbole) und b) JWS8 (offene Symbole) für das IR_{50} und das $pIRIR_{225}$ Signal.

Equivalent Dose (D_e), fading rates and age estimates

Equivalent doses (D_e) have been measured using IR_{50} and $pIRIR_{225}$ for all samples, and $pIRIR_{290}$ for three samples. Table 3 summarises the equivalent doses, saturation of the signal, recycling ratio, dose recovery results, residual doses, g-values and the resulting luminescence ages for all samples. The equivalent doses (D_e) obtained using the IR_{50} are in the range of ~500–700 Gy for core JW3 except for sample JWT8 which gives a significantly higher dose of 871 ± 63 Gy. These De estimates give minimum (uncorrected for fading) age estimates between 113 ± 9 ka and 240 ± 20 ka. De values obtained for IR_{50} do not increase systematically with depth, and indicate that this signal is in field saturation (equilibrium between the accumulation of new charge and the loss by anomalous fading) at ~500 Gy. Similar results were obtained by Degering & Krbetschek (2007a) on two samples with a depth of 104.5 m and 122.5 m from core JW2 from Jungfernweiher. They applied a multiple aliquot additive dose (MAAD) protocol to the polymineral fine-grain fraction and obtained equivalent doses (De) of 441 ± 49 Gy and 517 ± 62 Gy. The D_0-values of all IRSL and post-IR IRSL signals are about ~500–600 Gy suggesting that doses up to about ~1000-1200 Gy can be measured. The equivalent doses obtained using $pIRIR_{225}$ from feldspar range from 846 ± 52 Gy to 1174 ± 64 Gy for core JW3, which is ~25–50% higher than those obtained using IR_{50}. The De values of $pIRIR_{225}$ increase with depth, but the values for the lowermost two samples are already in the range of $2D_0$. This suggests a minimum uncorrected age of ~200 ka for the youngest sample. De values for $pIRIR_{290}$ signal are only available for sample JWS 1 (1137 ± 17 Gy) and for sample JWS 8 (1373 ± 53 Gy); these values are ~15–25% higher than the equivalent doses (D_e) obtained using the $pIRIR_{225}$ and give minimum age estimates of ~260 ka for the youngest sample and ~390 ka for one of the two oldest samples of JW3. The ages increase with depth but the De values are in the range of or exceed $2D_0$. The uncorrected $pIRIR_{225}$ ages underestimate the uncorrected $pIRIR_{290}$ age estimates by about 25–30 % on average, presumably because the $pIRIR_{225}$ signals have to be corrected for fading. The ratio of the sensitivity-corrected natural signal to the laboratory saturation level was calculated for IR_{50}, $pIRIR_{225}$ and for $pIRIR_{290}$ signals, and average values of 0.58 ± 0.04, 0.79 ± 0.03 and 0.79 ± 0.01 for IR_{50}, $pIRIR_{225}$ and $pIRIR_{290}$ were obtained, respectively. Schmidt et al. (submitted) tested the $pIRIR_{290}$ protocol on polymineral fine grains from Serbian loess investigating the behavior of both IR_{50} and $pIRIR_{290}$ in material close to or in saturation with a focus on the relationship between field and laboratory saturation. They could demonstrate that field saturation is equal to laboratory saturation for $pIRIR_{290}$, i.e., the ratio of the natural signal to the laboratory saturation level is close to 1. These findings show that the measured samples are not yet in field saturation for $pIRIR_{290}$ signal. Sample JWT9 (Fig.5 a,b), which was taken from core JW2 was measured using IR_{50}, $pIRIR_{225}$ and $pIRIR_{290}$. The equivalent doses (D_e) obtained using IR50 are around 600 Gy, which is in the range of the field saturated results for JW3 using this signal. For pIRIR225 an equivalent dose (D_e) of 1041 ± 30 Gy was measured, which is in the range of $2D_0$. For $pIRIR_{290}$ an equivalent dose (D_e) could not be calculated as the natural signal lies very close to the saturation level; the ratio of the sensitivity-corrected natural signal to the laboratory saturation level is 0.99 ± 0.01 (n=3) indicating that this sample is in saturation. Therefore, only a minimum dose estimate of ~270 ka based on the $2D_0$ value (86% of saturation) can be derived (~1100 Gy).

The measured fading rates for IR_{50}, $pIRIR_{225}$ and $pIRIR_{290}$ are shown in Fig. 7. For IR_{50}, the g-values range from 3.64 ± 0.12%/decade to 4.79 ± 0.11%/decade, with an average of 4.09 ± 0.02%/decade, n = 21, and for the $pIRIR_{225}$ signal, from 2.1 ± 0.2%/decade to 3.3 ± 1.0%/decade, with an average of 2.55 ± 0.14%/decade, n = 21 (Fig. 8). These data suggest that $pIRIR_{225}$ fades by ~40% less than IR_{50}. For sample JWS1 a g-value of 0.5 ± 1.1%/decade for $pIRIR_{290}$ was obtained. Similar fading rates for the $pIRIR_{225}$ and $pIRIR_{290}$ are reported by Thiel et al. (this issue) for their polymineral fine-grain samples, although they measured lower fading rates for IR_{50}. The fading corrected age estimates for IR_{50} and $pIRIR_{225}$ are

E&G / Vol. 60 / No. 1 / 2011 / 105–115 / DOI 10.3285/eg.60.1.07

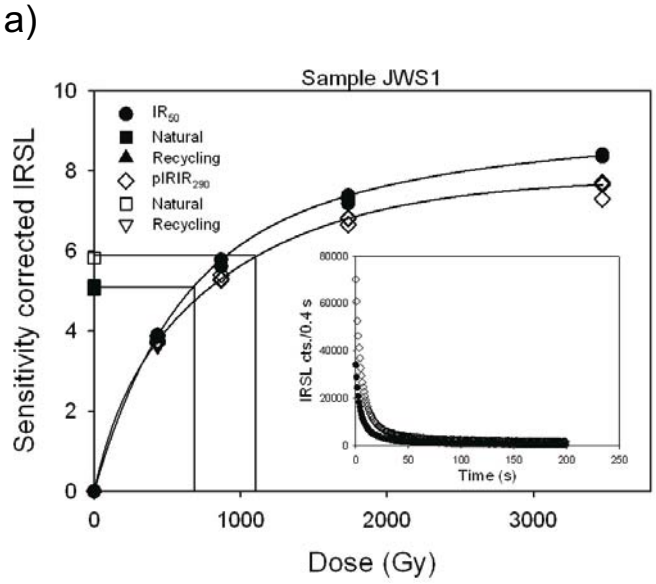

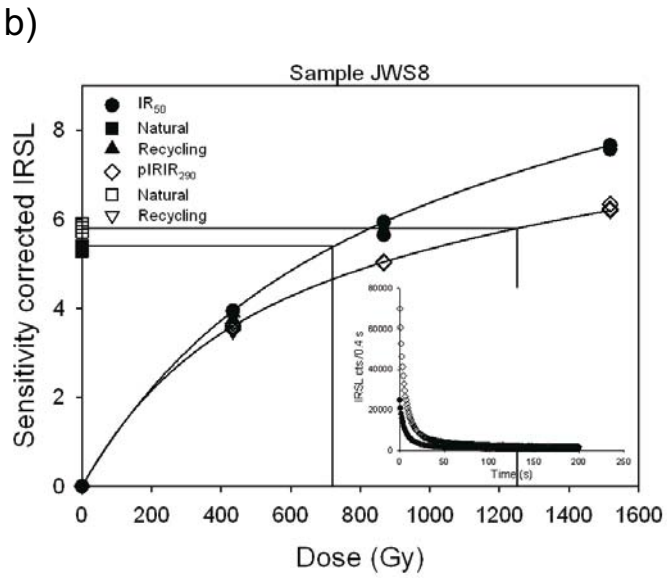

Fig. 4: Dose response and decay curves for sample a) JWS1 and b) JWT8 showing the IR_{50} (filled symbols) and the $pIRIR_{290}$ (open symbols).

Abb. 4: Aufbaukurve und Zerfallskurve für Proben a) JWS1 (gefüllte Symbole) und b) JWS8 (offene Symbole) für das IR_{50} und das $pIRIR_{290}$ Signal.

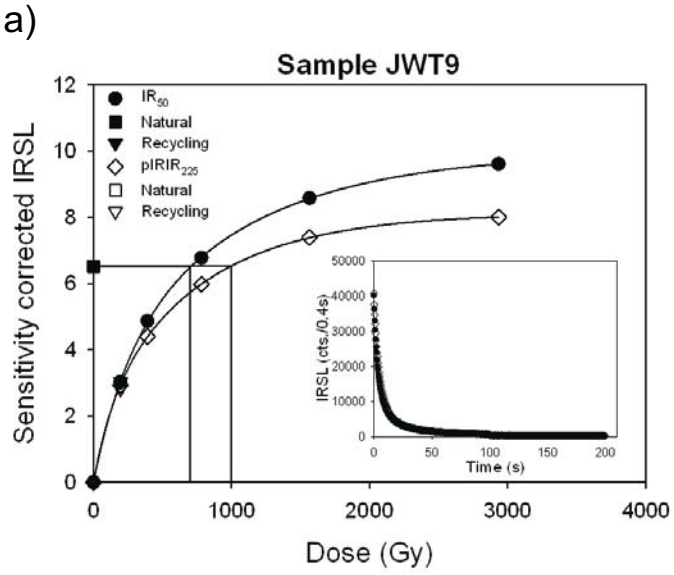

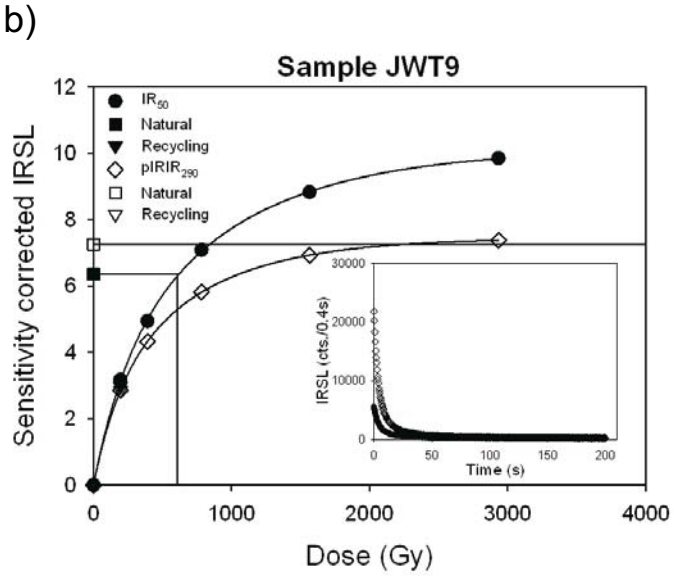

Fig. 5 a, b: Dose response and decay curves for sample JWT9 showing the IR_{50}, $pIRIR_{225}$ and the $pIRIR_{290}$.

Abb. 5 a, b: Aufbaukurve und Zerfallskurve für Probe JWT9 für das IR_{50}, das $pIRIR_{225}$ und das $pIRIR_{290}$ Signal.

listed in Table 3. The IR_{50} age estimates range from 188 ± 19 ka to 400 ± 80 ka. The age estimates for $pIRIR_{225}$ range from 270 ± 40 ka to >450 ka. The age estimates for $pIRIR_{290}$ are not fading corrected; Thiel et al. (2011) argue that fading rates below 1%/decade may not be significant, based on their finding of natural signals in saturation on a laboratory growth curve. The age estimates obtained for IR_{50} are consistently lower than those from $pIRIR_{225}$, except for sample JWT 3 and JWT 8. In contrast, our fading corrected $pIRIR_{225}$ age estimates are consistent with those from the uncorrected $pIRIR_{290}$. The underestimates from IR_{50} are consistent with the observation that this signal is in field saturation.

5 Discussion

Both $pIRIR_{225}$ and $pIRIR_{290}$ D_e values from the youngest sample (~16 m below modern surface) indicate a minimum (uncorrected for fading) age of ~200 ka for the deposits from Jungfernweiher. Fading corrected $pIRIR_{225}$ and uncorrected $pIRIR_{290}$ age estimates increase with depth from ~250 ka for the uppermost sample up to ~400 ka for the oldest samples taken ~94 m below modern surface indicating an accumulation of ~100 m over at least 150 ka. Thus according to post-IR IRSL ages, Jungfernweiher was effectively filled up with sediments ~250 ka ago, and there either has been very little deposition since then, or younger sediments have been eroded. However, there are uncalibrated radiocarbon age estimates ranging from 34.5 ± 2.1 ka BP to 56 ± 4 ka BP (no systematic increase with depth) which might indicate that these deposits are of late Weichselian age. Lenaz et al. (2010) also regard it as possible that the tephra layer at a depth of 107.39 m could be correlated with the Rocourt Tephra which has an age range between 90.3 and 74 ka. One possible explanation for our high D_e-values can be based on

Tab. 3: Summary of equivalent dose (D_e), saturation level, recycling ratio, dose recovery, residual doses, fading and luminescence ages. Six aliquots were measured per sample for dose determination. For the fading tests three aliquots/sample were measured.

Tab. 3: Äquivalenzdosen (D_e), Sättigungsniveau, Recycling Ratio, Dose Recovery, residuale Dosen, Fading und Lumineszenzalter. Sechs Aliquots wurden pro Probe für die Aquivalenzdosis-Bestimmung gemessen. Für die Fadingmessungen wurden drei Aliquots/Probe verwendet.

Sample	Depth	Measurement	De [Gy]	Saturation	Recycling	Measured/ given dose	Residuals [Gy]	g-value [%]	uncorrected Age [ka]	corrected Age [ka]
JWS1	16.60–16.62 m	IR50	527 ± 29	0.47 ± 0.02	0.96 ± 0.01	1.02 ± 0.003	2.49 ± 0.22	3.64 ± 0.12	124 ± 9	188 ± 19
		pIRIR225	846 ± 52	0.72 ± 0.04	0.98 ± 0.01	0.94 ± 0.05	3.92 ± 0.51	2.63 ± 0.34	199 ± 16	271 ± 35
		pIRIR290	1137 ± 17	0.79 ± 0.004	0.97 ± 0.01			0.52 ± 1.12	>270	
		OSL	441 ± 28		0.99 ± 0.02	0.97 ± 0.01			>100	
JWT3	18.54–18.56 m	IR50	686 ± 66	0.58 ± 0.03	0.99 ± 0.01	1.02 ± 0.13	2.21 ± 0.13	4.79 ± 0.11	154 ± 16	270 ± 31
		pIRIR225	921 ± 63	0.79 ± 0.03	0.97 ± 0.01	0.98 ± 0.03	5.54 ± 0.91	2.31 ± 0.48	207 ± 17	271 ± 44
		pIRIR290								
		OSL	523 ± 17		0.97 ± 0.01				>100	
JWT9	21.58–21.70 m	IR50	524 ± 30	0.41 ± 0.02	0.97 ± 0.02	1.04 ± 0.007		4.52 ± 0.23	113 ± 9	191 ± 28
		pIRIR225	936 ± 46	0.69 ± 0.03	0.97 ± 0.03	0.97 ± 0.04		3.33 ± 1.02	203 ± 14	297 ± 99
		pIRIR290								
		OSL								
JWT5	44.64–44.72 m	IR50	602 ± 26	0.6 ± 0.002	1.01 ± 0.07	1.10 ± 0.11	2.53 ± 0.04	4.35 ± 0.50	162 ± 12	271 ± 42
		pIRIR225	928 ± 38	0.79 ± 0.04	0.98 ± 0.01	0.99 ± 0.015	5.14 ± 0.63	2.45 ± 0.19	250 ± 18	336 ± 39
		pIRIR290								
		OSL								
JWT7	65.29–65.40 m	IR50	641 ± 37	0.65 ± 0.02	1.02 ± 0.02	1.12 ± 0.001	2.59 ± 0.02	3.98 ± 0.37	161 ± 12	258 ± 44
		pIRIR225	927 ± 61	0.87 ± 0.02	0.97 ± 0.01	1.00 ± 0.01	5.65 ± 0.28	2.51 ± 0.24	234 ± 20	316 ± 39
		pIRIR290								
		OSL	581 ± 54		0.98 ± 0.02				>100	
JWS8	93.12–93.15 m	IR50	598 ± 32	0.57 ± 0.03	0.96 ± 0.02	1.08 ± 0.002	2.84 ± 0.01	4.21 ± 0.43	170 ± 13	279 ± 41
		pIRIR225	1174 ± 64	0.86 ± 0.02	0.98 ± 0.02	0.96 ± 0.03	4.83 ± 0.03	2.48 ± 0.38	334 ± 25	>450
		pIRIR290	1373 ± 53	0.78 ± 0.03	0.98 ± 0.01				>390	
		OSL								
JWT8	93.73–93.83 m	IR50	871 ± 63	0.75 ± 0.05	0.98 ± 0.02	1.04 ± 0.01	2.52 ± 0.26	4.15 ± 0.61	243 ± 22	397 ± 79
		pIRIR225	1143 ± 49	0.86 ± 0.01	0.95 ± 0.01	1.02 ± 0.02	4.97 ± 0.23	2.11 ± 0.21	319 ± 21	>410
		pIRIR290								
		OSL								
JWT9 (core JW2)	104.5–104.6 m	IR50	600 ± 24	0.65 ± 0.01	0.99 ± 0.02				149 ± 10	
		pIRIR225	1041 ± 30	0.87 ± 0.01	0.98 ± 0.01				259 ± 15	
		pIRIR290 OSL	> 930*	0.99 ± 0.01	0.97 ± 0.01				>270	

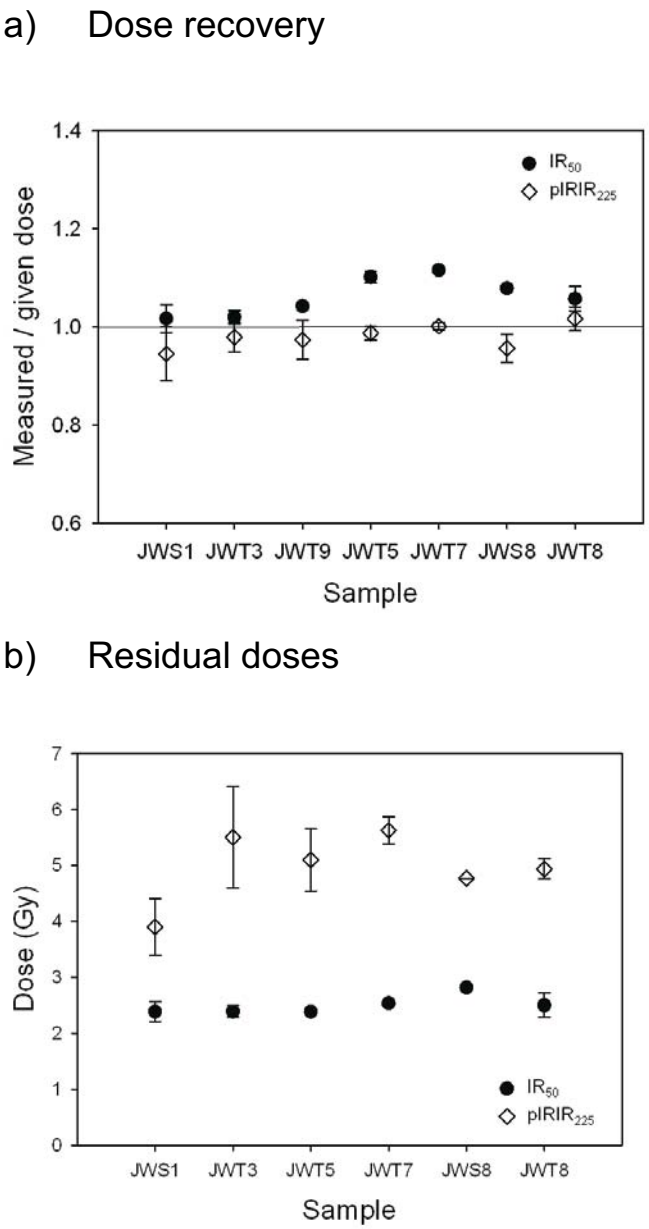

Fig. 6: Dose recovery test (a) and the residual doses (b) for the IR_{50} and the $pIRIR_{225}$ signal for all samples. Three aliquots were measured per sample. Error bars represent 1-sigma standard error.

Abb. 6: Dose recovery test (a) und residuale Dosen (b) für das IR_{50} und das $pIRIR_{225}$ Signal für alle Proben. Drei Aliquots wurden pro Probe gemessen. Die Fehlerbalken stellen den 1-sigma Standardfehler dar.

mixing of well-bleached aeolian dust with locally eroded old (field saturated) crater-wall sediment – then the sediment would have been deposited with an average finite residual dose, perhaps close to saturation. However, a simple mixing model indicates that for such a mixture to have been deposited at, say, ~20 ka, one would require >75% of the total lake sediment to be locally-derived old material in order to give a dose indistinguishable from field saturation today. Such a large catchment input to a maar lake seems very unlikely. Overestimated D_e-values could, of course, also arise because of incomplete bleaching. However, it seems most likely that the laminated coarser dust-storm and loess layers were deposited during high-glacial times; if such aeolian dust is making up a very large part of the sediment inventory it is difficult to accept that the IRSL is not well-bleached. There is considerable evidence in the literature that the IR_{50} from loess and from sediments originating from dust storms is well bleached (Roberts, 2008). It is also known that the fast component of quartz can be depleted in only a few minutes exposure to daylight (Godfrey-Smith et al., 1988) and yet we still obtain an equivalent dose for the fine-grain quartz of 441 ± 28 Gy giving a minimum age estimate of ~100 ka based on the $2D_0$ value of ~260–300 Gy for the youngest sample. Finally, a study from a nearby East Eifel crater fill (Schmidt et al, 2011) showed that the pulsed $pIRIR_{150}$ from loess deposits in this area is in fact well bleached. Their luminescence age estimates are in good agreement with stratigraphic evidence and with independent age control provided by $^{40}Ar/^{39}Ar$ dating of intercalated air-fall tephra and scoria. Thus we appear to have a discrepancy between the established stratigraphy and all IRSL data. Most of the radiocarbon ages are in the range of ~43–55 ka (except for one of ~35 ka) which is at or close to the upper age limit of the method. Luminescence age estimates are provided by Degering & Krbetschek (2007a) on two samples with a depth of 104.5 m and 122.5 m from core JW2 yielding equi-valent doses (D_e) of 441 ± 49 Gy and 517 ± 62 Gy. Age estimates of 98 ± 15 ka and 117 ± 18 ka were calculated for these samples. To enable comparison of our results for samples from the drill core JW3 and the published age estimates of Degering & Krbetschek (2007a) we additionally measured one sample (JWT9) from drill core JW2 taken from a depth of 104.5 m. The results show that this sample is in saturation for all the different signals, IR_{50}, $pIRIR_{225}$ and for $pIRIR_{290}$ suggesting a minimum age estimate of ~270 ka for $pIRIR_{290}$ signal for this sample. The calculated age estimates of Degering & Krbetschek (2007a) are underestimating our results significantly. One possible reason might be field saturation of their signal, i.e. the trap filling and anomalous fading had reached to the equilibrium state. In addition, the association of the tephra at 107 m with the Rocourt Tephra is not secure. In our view the post-IR IRSL ages represent the most secure ages for this deposit. It has to be mentioned, that one co-author (F.Sirocko) does not agree with this interpretation and proposes an alternative stratigraphy for core JW3 and neighbouring core JW2 (see appendix).

6 Conclusion

We have investigated the application of luminescence dating to maar lake sediments from the dry maar Jungfernweiher in the West Eifel volcanic field by using quartz OSL and two different protocols for feldspar IRSL. Using OSL, we obtained D_e values ranging from 440 ± 30 Gy to 580 ± 40 Gy for the fine-grain quartz extracts.All these results exceed the 2D0 value of ~260–300 Gy corresponding to minimum ages of ~80–100 ka (although the laboratory growth curve does not fully saturate before ~1000 Gy). For polymineral fine-grains, the D_e values obtained for IR_{50} do not increase with depth, and indicate that this signal is in field saturation at ~500 Gy. The D_e values for $pIRIR_{225}$ and $pIRIR_{290}$ are increasing with depth from ~800 Gy to ~1400 Gy, suggesting a minimum age of ~200 ka for the youngest material, although the obtained equivalent doses (D_e) are already in the range or exceeding $2D_0$ for two bottom samples for JW3 and the sample from JW2. Mean laboratory fading rates are 4.09 ± 0.02%/decade for IR_{50} and 2.55 ± 0.14%/decade for $pIRIR_{225}$.

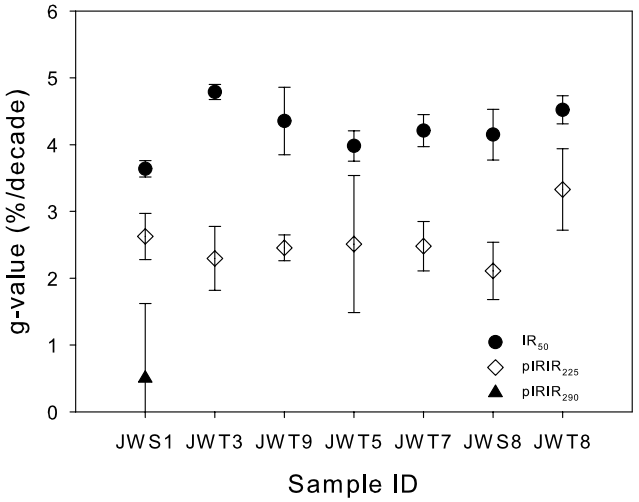

Fig. 7: Fading rates for the post the IR_{50} and $pIRIR_{225}$ signals for all samples. Three aliquots were measured per sample. Error bars represent 1-sigma standard error.

Abb. 7: Fadingraten für das IR_{50} und das $pIRIR_{225}$ Signal für alle Proben. Drei Aliquots wurden pro Probe gemessen. Die Fehlerbalken stellen den 1-sigma Standardfehler dar.

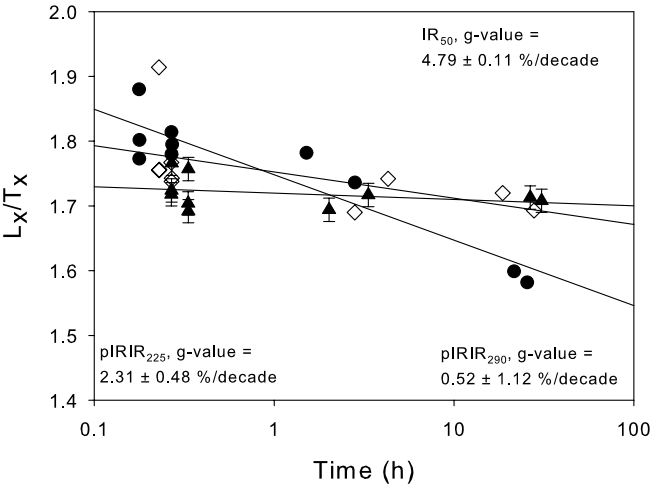

Fig. 8: Anomalous fading of $IRSL_{50}$, $pIRIR_{225}$ and $pIRIR_{290}$ signals.

Abb. 8: Anomalous fading für $IRSL_{50}$, das $pIRIR_{225}$ und das $pIRIR_{290}$ Signal.

Although we observed a g-value of 0.52 ± 1.12%/de-cade for $pIRIR_{290}$ from sample JWS1, we have chosen not to correct the age estimates for $pIRIR_{290}$ for fading. Corrected age estimates for $pIRIR_{225}$ range from 270 ± 40 ka to >450 ka. These ages are consistent with uncorrected $pIRIR_{290}$ age estimates. Not surprisingly, fading corrected age estimates obtained for IR_{50} underestimate the fading corrected age estimates for $pIRIR_{225}$. However radiocarbon age estimates and a possible tephra association suggest that these dated deposits should be of late Weichselian age. Based on the results from a simple sediment mixing model and on the results from analyses of well-bleached aeolian material from the nearby East Eifel, it is not likely that the high D_e-values observed within this study could originate from mixing or incomplete bleaching. Therefore we regard the results from the luminescence measurements conducted within this study to represent the most reliable age estimates for the sediments from the Jungfernweiher. The discrepancy between the established stratigraphy and the IRSL data from this study remains to be explained.

Acknowledgements

This research is part of the PhD study of EDS in the framework of the "Leibniz Pakt für Forschung und Innovation" at the LIAG-Institute in Hannover. EDS wishes to thank all members of the Sedimentology group of the Institute of Geosciences at the Johannes Gutenberg University in Mainz for their timely help, especially Stephan Dietrich, Klaus Schwibus and Frank Dreher. Christopher Lüthgens and an anonymous reviewer are thanked for the useful comments on the manuscript.

References

Adamiec, M. & Aitken, M.J. (1998): Dose-rate conversion factors: update. – Ancient TL 16: 37–50.

Aitken, M.J. (1985): *Thermoluminescence* Dating, London.

Aitken, M.J. (1998): An Introduction to Optical Dating, Oxford.

Auclair, M., Lamothe, M. & Huot, S. (2003): Measurement of anomalous fading for feldspar IRSL using SAR. – Radiation Measurements 37: 487–492.

Büchel, G. (1984): Die Maare im Vulkanfeld der Westeifel, ihr geophysikalischer Nachweis, ihr Alter und ihre Beziehung zur Tektonik der Erdkruste. – PhD-Thesis, Univ. Mainz, 385 pp.

Buylaert, J.P., Murray A.S. & Huot S. (2008): Optical dating of an Eemian site in Northern Russia using K-feldspar. Radiation Measurements 43: 715–720.

Buylaert, J.P., Murray, A.S., Thomson, K.J. & Jain, M. (2009): Testing the potential of an elevated temperature IRSL signal from K-feldspar. – Radiation Measurements 44: 560–565.

Buylaert, J.P., Huot, S., Murray, A.S. & Van den haute, P., in press. Infrared stimulated luminescence dating of an Eemian (MIS 5e) site in Denmark using K-feldspar. – Boreas, 10.1111/j.1502-3885.2010.00156.x.

Buylaert, J.P., Vandenberghe, D., Murray, A.S., Huot, S., De Corte, F. & Van den haute, P. (2007): Luminescence dating of old (>70 ka) Chinese loess: a comparison of single-aliquot OSL and IRSL techniques. – Quaternary Geochronology 2: 9–14.

Degering, D. & Krbetschek, M. R. (2007a): Dating of Interglacial Deposits by Luminescence Methods. – In: Sirocko et al. (Eds.): The Climate of Past Interglacials, Elsevier: 157–172.

Degering, D. & Krbetschek, M. R. (2007b): Lumineszenzdatierungen an limnischen Sedimenten von Klinge/Kreis Forst. – Natur und Landschaft: 120–128.

Duller, G.A.T. (2003): Distinguishing quartz and feldspar in single grain luminescence measurements. – Radiation Measurement 37: 161–165.

Duller, G.A.T. (2004): Luminescence dating of quaternary sediments: recent advances. – Journal of Quaternary Science 19(2): 183–192.

Frechen, M. (1991): Systematic thermoluminescence dating of two loess profiles from the middle Rhine area (F.R.G.). – Quaternary Science Reviews 11: 93–101.

Godfrey-Smith, D.I., Huntley, D.J. & Chen, W.-H. (1988): Optical dating of quartz and feldspar extracts. – Quaternary Science Reviews 7: 373–380.

Huntley, D.J. & Lamothe, M. (2001): Ubiquity of anomalous fading in K-feldspars and the measurement and correction for it in optical dating. – Canadian *Journal* of *Earth* Sciences 38: 1093–1106.

Lamothe M., Auclair M., Hamzaoui C. & Huot S. (2003): Towards a prediction of long-term anomalous fading of feldspar IRSL. – Radiation Measurements 37: 493–498.

Lang, A. & Zolitschka, B. (2001): Optical dating of annually laminated lake sediments A test case from Holzmaar/Germany. – Quaternary Science Reviews 20: 737–742.

Lenaz, D., Marciano, R., Veres, D., Dietrich, S. & Sirocko, F. (2010): Mineralogy of the Dehner and Jungfernweiher maar tephras (Eifel, Germany). – N.Jb.Geol.Palaont.Abh. Fast track DOI 10.1127/0077-7749/2010/0062.

Lowick, S., Preusser, F., Wintle, A. (2010a): Investigating quartz optically stimulated luminescence dose-response curves at high doses. –Radiation Measurements 45: 975–984.

Lowick, S.E., Preusser, F., Pini, R. & Ravazzi, C. (2010b): Underestimation of fine grain quartz OSL dating towards the Eemian: comparison with palynostratigraphy from Azzano Decimo, northeastern Italy. –Quaternary Geochronology 5: 583–590.

Murray, A.S., Buylaert J.P., Thomsen, K.J. & Jain M. (2009): The effect of preheating on the IRSL signal from feldspar. – Radiation Measurements 44: 554–559.

Murray, A.S. & Wintle, A.G. (2003): The single regenerative dose protocol: potential for improvements in reliability. – Radiation Measurements 37: 377–381.

Murray, A.S. & Olley, J.M. (2002): Precision and accuracy in the optically stimulated luminescence dating of sedimentary quartz: a status review. – Geochronometria 21: 1–16.

Negendank, J.F.W. & Zolitschka, B. (1993): Maars and maar lakes of the Westeifel volcanic field. In: J.F.W. Negendank and B. Zolitschka (Editors), Paleolimnology of European Maarlakes. – Lecture Notes in Earth Sciences. Springer-Verlag: 61–80.

Pouclet, A., Juvigné, E. & Pirson, S. (2008): The Rocourt Tephra, a widespread 90-74 ka stratigraphic marker in Belgium. – Quaternary Research 70: 105–120.

Prescott, J.R. & Hutton, J.T. (1994): Cosmic ray contribution to dose rates for luminescence and ESR dating: large depths and long-term time variations. – Radiation Measurements 23: 497–500.

Prescott, J.R. & Stephan, L.G. (1982): The contribution of cosmic radiation to the environmental dose for thermoluminescence dating. – PACT 6: 17–25.

Rees-Jones, J. (1995): Optical dating of young sediments using fine-grain quartz. – Ancient TL 13: 9–14.

Roberts, H.M. (2008): The development and application of luminescence dating to loess deposits: a perspective on the past, present and future. – Boreas 37: 483–507.

Schaber, K. & Sirocko, F. (2005): Lithologie und Stratigraphie der spätpleistozänen Trockenmaare der Eifel. – Mainzer geowiss. Mitt. 33: 295–340.

Sirocko, F., Seelos, K., Schaber K., Rein, B., Dreher, F., Diehl, M., Lehné, R., Jäger, K., Krbetschek, M. & Degering, D. (2005): A Late Eemian Aridity Pulse in central Europe during the last glacial inception. – Nature 436: 833–836.

Schmidt, E.D., Murray, A.S., Stevens, T., Buylaert, J.P., Marković, S.B., Tsukamoto, S. & Frechen, M., submitted. Elevated temperature IRSL dating of the lower part of the Stari Slankamen loess sequence (Vojvodina, Serbia) – investigating the saturation behaviour of the pIR-IR290 signal. – Quaternary Geochronology.

Schmidt, E.D., Frechen, M., Murray, A.S., Tsukamoto, S. & Bittmann, F. (2011): Luminescence chronology of the loess record from the Tönchesberg section – a comparison of using quartz and feldspar as dosimeter to extend the age range beyond the Eemian. – Quaternary International 234: 10–22.

Schmidt, E.D., Machalett, B., Marković, S. B., Tsukamoto, S. & Frechen, M. (2010): Luminescence chronology of the upper part of the Stari Slankamen loess sequence (Vojvodina, Serbia). – Quaternary Geochronology 5: 137–142.

Thiel, C., Buylaert, J.P., Murray, A.S., Terhorst, B., Hofer, I., Tsukamoto, S. & Frechen, M. (2011): Luminescence dating of the Stratzing loess profile (Austria) – Testing the potential of an elevated temperature post-IR IRSL protocol. – Quaternary International 234: 23–31.

Thiel, C., Buylaert, J.P., Murray, A.S., Terhorst, B., Tsukamoto, S. & Frechen, M. this issue. The chronostratigraphy of prominent palaeosols in Lower Austria: testing the performance of two post-IR IRSL dating protocols. – Eiszeitalter und Gegenwart.

Timar, A., Vandenberghe, D., Panaiotu, E.C., Panaiotu, C.G., Necula, C., Cosma, C. & Van den haute, P. (2010): Optical dating of Romanian loess using fine-grained quartz. – Quaternary Geochronology 5: 143–148.

Thomsen, K.J., Murray, A.S., Jain, M. & Bøtter-Jensen, L. (2008): Laboratory fading rates of various luminescence signals from feldspar-rich sediment extracts. – Radiation Measurements 43: 1474–1486.

Visocekas, R. (1985): Tunnelling radiative recombination in labradorite: Its association with anomalous fading of thermoluminescence. – Nuclear Tracks and Radiation Measurements 10 (4–6): 521–529.

Wintle, A. G. & Murray, A. S. (2006): A review of quartz optically stimulated luminescence characteristics and their relevance in single-aliquot regeneration dating protocols. – Radiation Measurements 41: 369–391.

Wintle, A.G. (1973): Anomalous fading of thermoluminescence in mineral samples. – Nature 245, 143–144.

Appendix

One of the co-authors (Frank Sirocko) has a different chronostratigraphical interpretation, which he describes in detail in a paper under submission. F. Sirocko interprets the luminescence dates from this study as result of a mixture of an eolian fraction with grains from the wave-generated erosion of soil material, which is again a mixture from the Devonian bedrock and loess of MIS6 or older.

According to Sirocko et al. (unpublished) the stratigraphical framework for JW2 and JW3 is as follows:

Scoria from the Laacher See eruption is apparent in the soil at 1 m depth, correlating to an eruption age of about 12.9 ka. Sediments from 1–22 m are free of clay and are regarded as a mixture from eolian deposition and wave generated suspensions. These sediments are free of pollen and correlate to the last glacial maximum (LGM). The relative paleointensity variation of sediment magnetisation places the Mono Lake Event at 24 m indicating an age of 30 ka according to the GLOPIS paleomagnetic stack, which is based on a GISP2 derived age model. A tuning of the greyscale variations between 25 and 41 m reproduces almost perfectly the succession of the Greenland Interstadials GI3–17. The second minimum of the relative paleointensity is at 32.5 m and correlates most likely to the Laschamps Event. The MIS3 sections of JW2 and JW3 have been studied by several ^{14}C dates giving ages around 50 ka representing the upper dating limit of the ^{14}C method. This would imply that all organic particles in JW3 are derived from soils of GI14, which was the warmest period of MIS3.

The markers of MIS5 start with a prominent step in the paleomagnetic inclination record at 81 m representing a principle change that was dated in the Monticchio record to 75 ka. The end of this inclination maximum is at 99 m, representing 86 ka. A tephra consisting of the same geochemical composition as the Roucourt tephra in France is visible in JW3 at 107.4 m, which would place this depth at around 90 ka. The sediments below yield two IRSL ages of 93 ka and 100 ka (Degering & Krbetschek, 2007a). The greyscale record between 75 m and 130 m can be perfectly tuned to the Greenland ice core stadial/interstadial succession and also the North Atlantic C-events. A tephra with an identical zonation to the Dümpelmaar tephra is visible at 139 m; this tephra was dated at the Herchenberg section to 116±10 ka. The succession of the markers of core JW3 ends with the occurrence of interglacial pollen at depth below 145 m most likely representing the Eemian.